LWT - Food Science and Technology 184 (2023) 115008

Contents lists available at ScienceDirect

LWT

journal homepage: www.elsevier.com/locate/lwt

Effects of microwave, ultrasound, and high-pressure homogenization on the physicochemical properties of sugarcane fibre and its application in white bread

Zawanah Abdol Rahim Yassin [a], Fatin Natasha Binte Abdul Halim [a], Afsaneh Taheri [a], Kelvin Kim Tha Goh [b], Juan Du [a,*]

[a] Food, Chemical and Biotechnology Cluster, Singapore Institute of Technology, 10 Dover Drive, Singapore, 138683, Singapore
[b] School of Food & Advanced Technology, Massey University, Private Bag 11222, Palmerston North, 4410, New Zealand

ARTICLE INFO

Keywords:
Glycemic response
Sugarcane fibre
Physical modification
In vitro digestion
Physicochemical properties
Bread

ABSTRACT

Sugarcane fibre (SCF) is known as an insoluble dietary fibre and a by-product from sugar manufacturing industry. The physicochemical and structural properties of SCF were modified using microwave irradiation at 5% and 10% SCF for 5 and 10 min ($MW_{5\%,15m}$, $MW_{10\%,5m}$, $MW_{10\%,15m}$), ultrasound at 30% amplitude, 7% SCF, for 1.5 h or 3 h (US_{1h}, US_{2h}), and high-pressure homogenization at 1% SCF, 2000 bar for 1 and 2 passes (HPH_{1p}, HPH_{2p}). Different types of disruption on the morphology of SCF were observed with different physical treatments confirmed by scanning electron microscopy. HPH_{2p} treated SCF exhibited the largest particle size, and highest water and oil-holding capacities. Fourier-transform infrared spectroscopy results showed that all physical treatments were able to reduce hemicellulose and enhance cellulose content in SCFs, especially for HPH treatments. After making dough and bread with treated and untreated SCF, HPH_{2p} SCF incorporated bread had the firmest texture, followed by $MW_{10\%,15m}$, while these two samples have the lowest specific volume. The maximum height of bread was significantly lower in breads incorporated with HPH_{2p}, $US_{1.5h}$ and US_{3h}. Subsequently, glycemic response decreased in all SCF-incorporated breads compared to white bread reference.

1. Introduction

There is an increasing concern associated with the prevalence of diet-dependent diseases that are often closely associated with chronic conditions of elevated insulin and blood glucose levels (Borczak et al., 2018; Burton et al., 2011). A strong correlation reportedly exists between diets that invoke a high glycemic response and the risk of developing Type 2 diabetes (Burton et al., 2011; Vlachos et al., 2020). With prolonged exposure to high blood glucose, a possibility exists that the body loses control over blood glucose levels and/or develops resistance to insulin, resulting in systemic damage over time. If left unmanaged, this may cause numerous disorders such as kidney failure and circulatory problems (Burton et al., 2011; Mishra et al., 2012). These are risk factors that can affect other conditions such as cardiovascular disease and cancer (Baena-Díez et al., 2016; Tseng, 2004). To counter these problems, previous studies have proposed to decrease dietary postprandial glycemic response (Borczak et al., 2018; Livesey et al., 2008).

White bread, a staple food, is commonly described with a high Glycemic Index (GI) (>70) (Atkinson et al., 2008; Borczak et al., 2018). Notably, it contains highly gelatinized starch and an open porous matrix which enables the rapid penetration of digestive enzymes (Burton et al., 2011; Monro et al., 2011). As the body quickly digests and absorbs the available carbohydrates in white bread, an elevated blood glucose level occurs after ingestion (Scazzina et al., 2013). Therefore, numerous methods have been proposed to effectively reduce postprandial glycaemia in bread, such as the addition of fibres into the bread (Borczak et al., 2018; Ellis et al., 1995; Scazzina et al., 2013), the development of a denser food matrix (Burton et al., 2011; Monro et al., 2011; SRV et al., 2019), and the addition of phenolic compounds (Kim et al., 2016; Lin et al., 2016). However, by adding dietary fibre into the bread structure, issues like reduced loaf volume, compacted bread crumb and decreased consumer acceptance were observed (Abdullah et al., 2021; Cavella et al., 2008; Miś et al., 2012). For instance, adding potato fibre resulted in the deterioration of loaf volume (Kaack et al., 2006; Lu et al., 2021), due to a decrease in gas retention ability from gluten dilution (Han et al., 2018). This has also been observed with the incorporation of partially

* Corresponding author.
E-mail address: du.juan@singaporetech.edu.sg (J. Du).

https://doi.org/10.1016/j.lwt.2023.115008
Received 9 April 2023; Received in revised form 18 June 2023; Accepted 22 June 2023
Available online 23 June 2023

hydrolyzed guar gum (Mudgil et al., 2016), sugarcane bagasse (Sangnark & Noomhorm, 2004), blackcurrant fibre (Alba et al., 2020), as well as carob fibre, pea fibre and inulin (Wang et al., 2002).

Also, an overall increase in water absorption by dough has been reported when fibre is added, which can be attributed to the presence of numerous hydroxyl groups in the fibre structure that allows interactions with water molecules via hydrogen bonding (Ahmed et al., 2013; Miś et al., 2012; Mudgil et al., 2016; Ognean, 2015). Furthermore, the incorporation of insoluble fibre, such as in lignocellulosic materials, has reportedly resulted in poor integration into the dough matrix due to weak hydration (Gould et al., 1989). Thus, physical, chemical, or enzymatic modification methods have been suggested to improve water solubility, and subsequently the functionality of lignocellulosic materials. A general mechanism of action involves the disruption of hydrogen bonds in the crystalline cellulose structure and breakdown of the cross-linked matrix, consisting of hemicellulose and lignin. This increases the porosity and surface area of cellulose, thereby exposing free hydroxyl groups that can interact with water molecules via hydrogen bonding (Gould et al., 1989; Mood et al., 2013). Modification methods are mainly classified as chemical, physical and biological (Mood et al., 2013; Rabemanolontsoa & Saka, 2016). In this study, we focused on 3 different modification methods of physical nature: microwave irradiation, ultrasonication, and micronization.

Microwave irradiation is a process that involves the conversion of electromagnetic energy to thermal energy, resulting in heating via molecular interaction in the presence of a magnetic field (Brahim et al., 2016). On the other side of the spectrum, ultrasound is a series of expansion and compression cycles of air bubbles that are induced in the liquid medium, leading to pressure inside the air bubbles that reach values as high as 50 MPa, and can generate intense heat. This is described as the cavitation phenomena and brings damage to the biomass matrix (Brahim et al., 2016). The application of microwave and ultrasound on wheat bran at different temperatures and through a variety of durations (Brahim et al., 2016) showed that a longer treatment time improved delignification yields from 28.3% to 28.6% in 10 min, and from 38.4% to 41.5% in 40 min, by the effect of microwave and ultrasound, respectively. The delignification yield also increased in response to higher temperature in the ultrasound treatment. Micronization includes microfluidization and high-pressure homogenization. In particular, there are indications that microfluidization may involve the partial rupturing of cells and the destruction of macromolecular structures due to fluid shear stress in wheat bran (Wang et al., 2012) as well as peach and oat fibre (Chen et al., 2013). This has reportedly caused a significant decrease in particle size and an increase in particle porosity, while improving swelling capacity, water holding capacity and oil holding capacity (Chen et al., 2013; Rosa-Sibakov et al., 2015; Wang et al., 2012).

In this study, the objectives include evaluating the physicochemical and structural properties of SCF that were modified using microwave irradiation, ultrasound, and high-pressure homogenization at different conditions and parameters, and determining the effects of incorporating modified SCF on the physical properties and *in vitro* glycemic response of white bread.

2. Materials and methods

2.1. Materials and reagents

Amyloglucosidase (EC 3.2.1.3 from *A. niger*, Megazyme, E-AMGDF; 3260 U/Ml) was purchased from Megazyme. Absolute ethanol, 37% HCl, and glacial acetic acid were purchased from MERCK (Singapore). NaOH pellets, 99% ethanol, and sodium bicarbonate were purchased from AIK MOH (Singapore). D-(+)-Glucose, sodium dodecyl sulfate, pepsin (pepsin EC 3.4.23.1 from porcine gastric mucosa, P7000, Sigma-Aldrich, USA; USP ≥250 U/mg), pancreatin (EC 232-468-9 from porcine pancreas, P7545, Sigma-Aldrich, USA; USP x 8 specifications), invertase (EC 3.2.1.26 from *S. cerevisiae*, I4504, Sigma-Aldrich, USA; ≥300 U/mg), maleic acid, sodium azide, calcium chloride dihydrate, sodium acetate, potassium sodium tartrate and 3,5-dinitrosalicylic acid were purchased from Sigma Aldrich (Singapore).

2.2. Physical treatments of SCF

2.2.1. Microwave irradiation

MW pre-treatment was modified from Agu et al. (2017). SCF (5% w/w and 10% w/w) were dispersed in deionized water in a beaker and irradiated in a microwave oven (MC28H5015AS, Samsung, South Korea) at 450 W for 5 and 15 min. 3 different treatment conditions were used in the study, namely $MW_{5\%,15m}$ (5% w/w, 15 min), $MW_{10\%,5m}$ (10% w/w, 5 min), and $MW_{10\%,15m}$ (10% w/w, 15 min). Mixtures were taken out every 2.5 min to be stirred. Subsequently, mixtures were cooled to room temperature and centrifuged (Eppendorf centrifuge 5424R, Eppendorf GMBH, Germany) at 4000 *g* for 10 min. The supernatant was decanted, and the pellets were rinsed, frozen at −80 °C for 24 h and freeze dried (VirTis Benchtop Pro, SP Scientific, USA) at −80 °C for at least 72 h under vacuum condition for further analysis.

2.2.2. Ultrasonication

US treatment of SCF was modified from Shahi et al. (2020), where 14 g of SCF was dispersed in 186 mL deionized water to make 7% (w/w) sample to mixture ratio. The mixture was ultrasonically irradiated for 1.5 and 3 h, labelled as $US_{1.5h}$ and US_{3h} respectively, with a 20 kHz frequency ultrasound processor (Sonics Vibra Cell VCX 750, USA) attached to a 13 mm diameter probe running at 30% amplitude and with 15 s on and 5 s off cycle. To prevent overheating of the system, the mixture was kept in an ice bath which was changed hourly. Subsequently, mixtures were centrifuged (Eppendorf centrifuge 5424R, Eppendorf GMBH, Germany) at 4000 *g* for 10 min. The supernatant was decanted, and the pellets were rinsed, frozen at −80 °C for 24 h and freeze dried (VirTis Benchtop Pro, SP Scientific, USA) at −80 °C for at least 72 h under vacuum condition for further analysis.

2.2.3. High pressure homogenization

SCF was dispersed (1% w/w) in deionized water and mixed, and the suspension was processed through a microfluidizer (M-110P, Microfluidics, United States) at 2000 bar for one and two passes, labelled as HPH_{1p} and HPH_{2p} respectively. Subsequently, mixtures were centrifuged (Eppendorf centrifuge 5424R, Eppendorf GMBH, Germany) at 4000 *g* for 10 min. The supernatant was decanted, and the pellets were rinsed, frozen at −80 °C for 24 h and freeze dried (VirTis Benchtop Pro, SP Scientific, USA) at −80 °C for at least 72 h under vacuum condition for further analysis.

2.3. Physicochemical properties of SCF

2.3.1. Particle size analysis

Particle size distribution of the fibre samples were analyzed with a laser light scattering particle analyzer (Malvern Mastersizer 3000, Malvern Instruments, United Kingdom) using the Mie scattering model. To ensure sufficient dispersion, samples were homogenized in 1% sodium dodecyl sulfate (SDS) solution at 3000 rpm for 2 min with a homogenizer (T18 digital Ultra-Turrax®, IKA®-Werke GmbH & Co.KG, Germany) fitted with an S18N-19G dispersing tool. Refractive indexes used for the sample and dispersant were 1.4683 for cellulose (Sultanova et al., 2009) and 1.33 for water respectively (Binte Abdul Halim et al., 2023). Each measurement was conducted in triplicate. $d_{4,3}$, $d_{3,2}$, and percentile volume-weighted diameter values at 10%, 50%, and 90% were reported.

2.3.2. Water holding capacity (WHC) and oil holding capacity (OHC)

WHC and OHC determination was modified from Zhao et al. (2023). 1 g of SCF and 20 mL of deionized water or canola oil was added to a

centrifuge tube and mixed thoroughly using a vortex mixer (Vortex-Genie 2; Scientific Industries, New York, USA) for 1 min at highest speed. The sample was left to sit for 2 h at room temperature. After which, the sample was centrifuged (Eppendorf centrifuge 5424R, Eppendorf GMBH, Germany) at 3000 *g* for 30 min at 25 °C for WHC or 1500 *g* for 10 min at 25 °C for OHC. Without disturbing the pellet, the supernatant was removed using a 3 mL plastic dropper. After the complete removal of excess water or oil, the centrifuge tube containing the sample was weighed. The procedure was repeated thrice. WHC or OHC of SCF was determined following Equation (1).

$$\text{WHC or OHC} = \frac{\text{wet weight} - \text{dry weight}}{\text{dry weight}} \quad \text{(Eq. 1)}$$

2.3.3. Scanning electron microscopy (SEM)

The effect of different types and extent of physical treatments on the surface morphology of the SCF samples were assessed with the use of a scanning electron microscope (JSM IT800, JEOL Ltd, Japan). Samples were mounted on a conductive carbon adhesive tape and sputtered with platinum (30 mA, 70 s) (Binte Abdul Halim et al., 2023).

2.3.4. Fourier transform infrared spectroscopy (FTIR)

A small amount of freeze-dried SCF sample was analyzed using an ATR FT-IR spectrophotometer (Agilent Cary 630 FTIR, Agilent Technologies, USA). The spectrum wavelength was recorded from 600 to 4000 cm^{-1} at a resolution of 4 cm^{-1} with 64 scans (Ameram et al., 2019). Data were processed by Origin® software and the normalization of spectra was initially made between 0 and 1. The secondary derivative was calculated within a spectral range of 600–4000 cm^{-1} (Binte Abdul Halim et al., 2023; Taheri et al., 2023).

2.4. Bread making

2.4.1. Dough formulation

Wheat flour, water, instant dry yeast, salt, and sugarcane fibre were the general constituents in the bread formulation. The flour (Pharaoh Flour, Prima, Singapore) contained approximately 72% carbohydrate, 12% protein, 0.40% ash and 14% moisture and was obtained from Prima while instant dry yeast (Saf-Instant, Lesaffre, France) was purchased from NTUC FairPrice Singapore (Table S1).

To ensure adequate flour hydration for optimal dough development, the water content of the formulations was determined with a prior farinograph analysis (doughLAB 2500, Perten Instruments, Sweden) which was based on the standard AACC International Method 54–21.02 (Rheological Behaviour of Flour by Farinograph: Constant Flour Weight Procedure). Briefly, 300 g of flour with or without 15 g of SCF was mixed at 30 °C and 63 rpm for 20 min while water was added via an automatic dripping system. The amount of water required to attain a torque (resistance to mixing) of 500 ± 25 Farinograph Units (FU) was recorded as the amount needed to obtain optimal dough strength (Binte Abdul Halim et al., 2023).

2.4.2. Bread preparation

Reference bread samples were prepared with 300 ± 1 g of wheat flour, 3.6 ± 0.1 g of dry yeast, 6 ± 0.1 g of salt, and 193.5 ± 0.5 g of water. SCF-incorporated bread samples were prepared with 300 ± 1 g wheat flour, 3.6 ± 0.1 g dry yeast, 6 ± 0.1 g salt, 15 ± 0.1 g of SCF, and 208.8 ± 0.5 g of water.

Bread samples were prepared according to the straight dough method (AACC International Method 10–09.01., 2009). Dough was prepared with the use of a stand mixer (KitchenAid 3.3L Artisan Mini Stand Mixer, USA) fitted with a spiral dough hook. Water required per formulation was first split to 20% and 80% portions, which were at room temperature (25 ± 2 °C) and chilled (4 ± 2 °C) conditions respectively. To further control dough temperature, chilled flour (4 ± 2 °C) was used. Dry yeast was dispersed and hydrated in the 20% room temperature portion of water for 5 min prior to form a yeast solution while dry ingredients were pre-mixed at speed 1 for 1 min. Subsequently, the yeast solution and chilled water portion were slowly added, and the mixing speed was increased to Speed 2 for 2 min and then to Speed 4 for another 9 min. The dough temperature was kept below 22 °C to control fermentation by yeast activity. This mixing condition was kept standardized across all bread formulations for consistency.

Next, the dough was removed from the mixer, covered, and left to rest under ambient conditions (25 ± 2 °C) for 5 min before it was split to two portions of 195 g each. Dough pieces were pre-shaped and proofed at 30 ± 2 °C and 85 ± 2% relative humidity (RH) for a total for 120 min. After 60 min of proofing, dough pieces were gently kneaded and shaped by hand to expel the gas evolved during fermentation and transferred into loaf pans (154 mm × 86 mm × 47 mm) before a second round for proofing for 60 min. Samples were then baked at 200 ± 2 °C for 30 min in a pre-heated oven (MC28H5015AS, Samsung, South Korea). Baked bread samples were left to cool on a rack for at least 1 h prior to further analysis. Each formulation was baked in two different batches.

2.5. Physical characterization of SCF-incorporated dough and bread

2.5.1. Dough extensibility

After mixing, 15 g of dough was immediately set aside for dough extensibility measurement as modified from Liu et al. (2017) using a texture analyzer (TA.XT Plus, Stable Micro Systems, UK) equipped with a 5 kg load cell and a Kieffer rig attachment. In preparation for extensibility measurement, the dough sample was first rolled and compressed in the Teflon mould and kept in refrigerated conditions for 30 min to slow down yeast activity while allowing the dough to rest before analysis. For this measurement, the dough samples were subjected to a tension test with a 5 g trigger force and 75 mm distance. Pre-test, test, and post-test speeds were set at 2, 3.3 and 10 mm/s respectively. Each measurement was conducted with 10–12 dough strips per batch. Resistance of extension is the force (g) required to pull at breaking point. Extensibility (mm) is the distance at which the dough string broke.

2.5.2. Maximum loaf height and specific loaf volume

The maximum loaf height was measured at the middle section of the bread samples with an electronic vernier caliper. Specific loaf volume was measured with a solid displacement method based on the standard AACC International Method 10–05.01. (2001) (Measurement of Volume by Rapeseed Displacement). In brief, a container was filled with seeds and the top surface was levelled. The bread samples were subsequently placed in the container, top surface levelled again, and the volume of seeds displaced was recorded as the loaf volume. Next, loaf volume (cm^3) measured was divided by loaf mass (g) to derive specific loaf volume (cm^3/g) of the respective loaf volumes. Each measurement was conducted in duplicate.

2.5.3. Texture Profile analysis (TPA)

The method for TPA of bread samples was modified from Liu et al. (2017). Bread samples were cut into 25 mm thick slices, surface area ranging from 4500 to 5000 mm^2, kept sealed in ziplock bags and stored in airtight containers at ambient conditions before analysis. Analysis was conducted a day after baking using a texture analyser (TA.XT Plus, Stable Micro Systems, UK) equipped with a 5 kg load cell and a 36 mm aluminium compression plate (P/36R, Stable Micro Systems, UK). The double compression test was at 5 g trigger force, 40% strain and 5 s between each compression cycle, with pre-test, test and post-test speeds at 1 mm/s, 2 mm/s and 2 mm/s respectively. Each measurement was conducted in triplicate. Hardness is recorded as the maximum force of the first compression. Chewiness is recorded as the energy required to chew solid foods (Binte Abdul Halim et al., 2023).

2.5.4. Moisture content determination

The moisture content of the bread samples was measured one day

after baking, whereby samples were kept sealed in Ziplock bags and stored in airtight containers at ambient conditions before analysis. 4 g of bread crumb sample was analyzed with a halogen moisture analyser (HE 53, Mettler Toledo, USA), heated to 105 °C under automatic operating conditions. Measurements were conducted in duplicate.

2.6. Determination of in vitro glycemic response

Glycemic response was determined with *in vitro* amylolysis of the bread samples, which measures the rate of glucose release in an *in vitro* system that stimulates the gastric peptic (non-amylolytic) phase at pH 2.5 followed by the small intestinal (amylolytic) phase at pH 6.5 (SRV et al., 2019). This *in vitro* model accounts for the adjustment of glycemic glucose equivalent (GGE) and corresponding blood glucose clearance relative to realistic food portions, thus reporting values comparable to *in vivo* blood glucose response (Monro et al., 2010).

Firstly, 5 g of bread sample, in dry weight basis, was added to 60 mL of deionized water and homogenized with an S18N-19G dispersing tool (T18 digital ULTRA-TURRAX®, IKA®-Werke GmbH & Co.KG, Germany) at 6000 rpm for 2 min. Only the crumb portion of the bread samples were used for a more representative analysis. The gastric phase was first stimulated by adjusting the sample mixture to pH 2.5 with 1 M HCl. Next, 2 mL of 10% (w/v) pepsin was added and the sample mixture was incubated in a water bath (SB-12l, Benchmark Scientific, USA) at 170 rpm and 37 °C for 30 min. The small intestinal phase was subsequently initiated by neutralising the gastric sample mixture with 4 mL of 1 M sodium bicarbonate and 10 mL of 0.1 M sodium maleate buffer (pH 6.0). A 0.5 mL aliquot (time zero sample) was transferred and thoroughly mixed in 2 mL of chilled absolute ethanol. To commence amylolysis of the sample, 0.2 mL of amyloglucosidase and 2 mL of 5% pancreatin dissolved in 0.1 M sodium maleate buffer were incorporated. Sample volume was topped up 110 mL with deionized water and incubated at 37 °C with continuous shaking at 170 rpm. Successive 0.5 mL aliquots were taken at 10, 20, 30, 40, 60, 120 and 180 min and thoroughly mixed in 2 mL chilled absolute ethanol. All inactivated aliquots were kept in refrigerated conditions prior to the quantification of glucose release. Duplicates of the timed samples were taken (Binte Abdul Halim et al., 2023).

2.7. Quantification of glucose release

The release of reducing sugars during the digestion process was measured using the dinitrosalicylic acid (DNS) colorimetric method as described by (Binte Abdul Halim et al., 2023; SRV et al., 2019). Inactivated aliquots were first centrifuged at 1000 *g* at 25 °C for 10 min to remove any particulate material. Next, 0.05 mL of the supernatant was transferred to 0.25 mL of enzyme solution containing 1% (v/v) amyloglucosidase and 0.05% invertase dissolved in 0.1 M sodium acetate buffer (pH 5.2). The mixture was incubated at 37 °C for 15 min to convert all saccharides to glucose. Subsequently, 0.75 mL of DNS mixture (comprising of a 1:1:5 mixture of 0.5 mg/mL of glucose solution, 4 M NaOH and DNS reagent respectively) was added, and the contents were heated at 95 °C for 15 min. Tubes were cooled in ice water and 4 mL of deionized water was added and thoroughly mixed. Absorbance of the mixtures were recorded at 530 nm (Cary 60 UV–Vis Spectrophotometer, Agilent Technologies, USA). To quantify the glucose content of SCF, absorbance values of the samples were compared against a glucose standard curve, which used glucose concentrations of 0, 1, 2.5, 5, 7.5 and 10 mg/mL and compared to deniozed water as a blank.

2.8. Data analysis for in vitro glycemic potency determination

Glucose release during *in vitro* digestion was quantified via the dinitroslicylic acid (DNS) colorimetricc method (Monro et al., 2010; SRV et al., 2019) using a glucose standard curve (y = 0.1003 x + 0.2051). The values were then used to calculate the glycemic glucose equivalent (GGE). GGE release curves were obtained by plotting the GGE values against the *in vitro* digestion time. The glucose disposal (GD) rate values were derived from Equation (2) and subsequently used to derive the GGE disposal per time point (GD × time point = GGE disposal). The values obtained were then plotted against the *in vitro* digestion time to depict the GGE disposal curves. Subsequently, to account for blood glucose clearance, the GGE disposal values were subtracted from the GGE release to generate net GGE values (Net GGE = GGE - GD). To account for the *in vivo* delay in the onset of the glycemic response, the *in vitro* digestion time was extended for an additional 10 min. These values were then plotted against the net GGE.

Table 1
Particle size of SCF samples with different treatments compared with untreated SCF.

Sample	$d_{3,2}$ (μm)	$d_{4,3}$ (μm)	d_{10} (μm)	d_{50} (μm)	d_{90} (μm)
Untreated	23.1 ± 1.2^{c}	40.4 ± 2.3^{cd}	11.7 ± 0.6^{cd}	31.4 ± 2.2^{c}	81.7 ± 4.3^{c}
$MW_{5\%,15m}$	20.8 ± 0.6^{cd}	37.5 ± 1.9^{cd}	11.3 ± 0.2^{d}	30.7 ± 1.0^{c}	74.2 ± 4.9^{cd}
$MW_{10\%,5m}$	20.9 ± 0.3^{cd}	42.0 ± 0.9^{c}	12.5 ± 0.1^{c}	34.4 ± 0.5^{c}	82.8 ± 2.2^{c}
$MW_{10\%,15m}$	19.3 ± 1.7^{d}	40.9 ± 0.9^{cd}	11.3 ± 0.3^{d}	33.1 ± 0.6^{c}	82.0 ± 2.1^{c}
$US_{1.5h}$	19.6 ± 0.0^{d}	37.7 ± 0.1^{d}	10.0 ± 0.1^{e}	29.8 ± 0.1^{c}	76.9 ± 0.2^{cd}
US_{3h}	19.3 ± 0.1^{d}	34.6 ± 1.0^{cd}	9.8 ± 0.1^{e}	29.5 ± 0.4^{c}	66.9 ± 3.9^{d}
HPH_{1p}	32.1 ± 0.4^{b}	71.2 ± 2.8^{b}	15.7 ± 0.1^{b}	55.0 ± 0.9^{b}	153.0 ± 8.7^{b}
HPH_{2p}	48.1 ± 2.1^{a}	118.0 ± 4.6^{a}	22.2 ± 1.0^{a}	99.5 ± 5.8^{a}	243.3 ± 8.4^{a}

Particle size values are expressed as mean ± SD (n = 3), where different superscript letters represent a significant difference ($p < 0.05$) in a column.

$$GD_{rate} = 0.0135GGE_x + 0.02232 \quad \text{(Eq. 2)}$$

where x = GGE released by 100 *g of bread at* 40 min *of in vitro digestion*

The incremental area under the curve (iAUC) was calculated based on the net GGE curve using the triangle/trapezoid summation method described by World Health Organization (WHO) (Monro et al., 2010). The relative glycemic potency (RGP) of bread samples was determined on an equal weight basis of 100 g of bread in comparison with the iAUC of a white bread reference of known GGE. The glycemic index (GI) of bread samples were then estimated by comparing the calculated iAUC of bread samples with the iAUC of reference bread (Eq. (3)).

$$GI_{bread\ sample} = \frac{iAUC\ of\ bread\ sample}{iAUC\ of\ reference} \times GI_{reference} \quad \text{(Eq. 3)}$$

2.9. Statical analysis

Statistical analyses were performed with one-way analysis of variance (ANOVA) test using Minitab software (Minitab®19). The means and standard deviation were compared using Tukey's honest significance test at 95% confidence level, where a significant difference is observed when $p < 0.05$. Analytical values of experiments are shown as mean ± standard deviation.

3. Results and discussion

3.1. Effects of physical modifications on the physicochemical properties of sugarcane fiber

All pre-treatment methods led to high yields – $MW_{5\%,15m}$ (92.5%), $MW_{10\%,5m}$ (93.3%), $MW_{10\%,15m}$ (93.1%), $US_{1.5h}$ (92.9%), US_{3h} (94.1%), HPH_{1p} (94.5%), HPH_{2p} (92.9%) – demonstrating favorable circumstances for potential industrial processing. The particle size (Table 1),

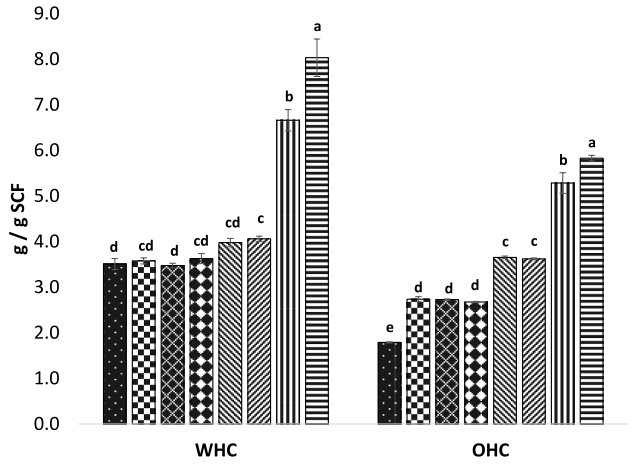

Fig. 1. WHC and OHC of untreated and treated SCF, different letters represent a significant difference among within each functional test. refers to Untreated SCF sample, refers to $MW_{5\%,15m}$, refers to $MW_{10\%,5m}$, refers to $MW_{10\%,15m}$, refers to $US_{1.5h}$, refers to US_{3h}, refers to HPH_{1p}, and refers to HPH_{2p}.

WHC and OHC (Fig. 1) of treated samples were compared to the untreated sample.

3.1.1. Particle size analysis

Table 1 demonstrates that there was significant difference among the treated samples for $d_{3,2}$, with US_{3h} displaying the smallest size. It is important to note that $d_{3,2}$ is more sensitive to smaller particles, whereas $d_{4,3}$ is more sensitive to larger particles. As the number of passes in HPH increased, $d_{4,3}$ increased, indicating the presence of small quantities of large particles (Serra et al., 2008). As shown in Table 1, the smallest difference between $d_{3,2}$ and $d_{4,3}$ was observed for $US_{1.5h}$ and US_{3h}. These results indicate that the apparent shape of SCF treated with ultrasound were more consistent than the other treatments (Wang et al., 2021), resulting in a more regular and uniform particle size distribution, which is desirable characteristics for many applications.

3.1.2. WHC and OHC

Fig. 1 depicts the WHC and OHC of untreated and treated SCF. WHC did not significantly increase with microwave and ultrasound treatment ($US_{1.5h}$) but significantly increased with longer ultrasonication time (US_{3h}) and high-pressure homogenization (HPH_{1p} and HPH_{2p}). With a longer ultrasonication time, this allowed for a more extensive destruction of the sample matrix, which meant an increase of exposure for hydroxyl groups that resulted in hydrogen bonding with water, thereby increasing WHC (Brahim et al., 2016). With high pressure homogenization, the loosening of the fibre microstructure could lead to cavity creation and could enable more water to be trapped by the structure (Wang et al., 2012). Additionally, the significant increase in WHC of high-pressure homogenization samples could be explained by the conversion of fiber particles from spherical to multi-branching flakes, probably resulting from an intense mechanical impact, and the release of the hydrophilic groups (Dickinson, 2018). After high pressure homogenization, water molecules and exposed hydrophilic groups acquired a greater level of contact area, thereby leading to an improvement in WHC.

Furthermore, all pre-treatments significantly improved OHC, but to varying degrees. HPH_{2P} had the most significant increase in OHC, followed by HPH_{1p}, ultrasonication and, lastly, microwave irradiation. The level of increasement differed due to the different mechanisms of treatment methods and the degree of disruption that the microstructure of fibres experienced. The surface of the fiber hosts many lipophilic groups, enabling the fiber particles to physically entrap oil (Ahmadi et al., 2019). The surface area, number of lipophilic groups, and the amount of oil correlate positively with the effectiveness of OHC. After high pressure homogenization, OHC of SCF increased because the particles appeared more like multi-branched flakes, compared to their previous spherical shape, leaving an abundance of small holes on the fiber surface (Zhu et al., 2018). In turn, this induced a larger surface area on SCF. A study conducted by (Hua et al., 2017) revealed that high pressure homogenization enhanced the OHC of fiber in tomato fruits. This can explain the reason behind significant increases that happened in the case of HPH_{1p} and HPH_{2p} as well. As for ultrasonication, the

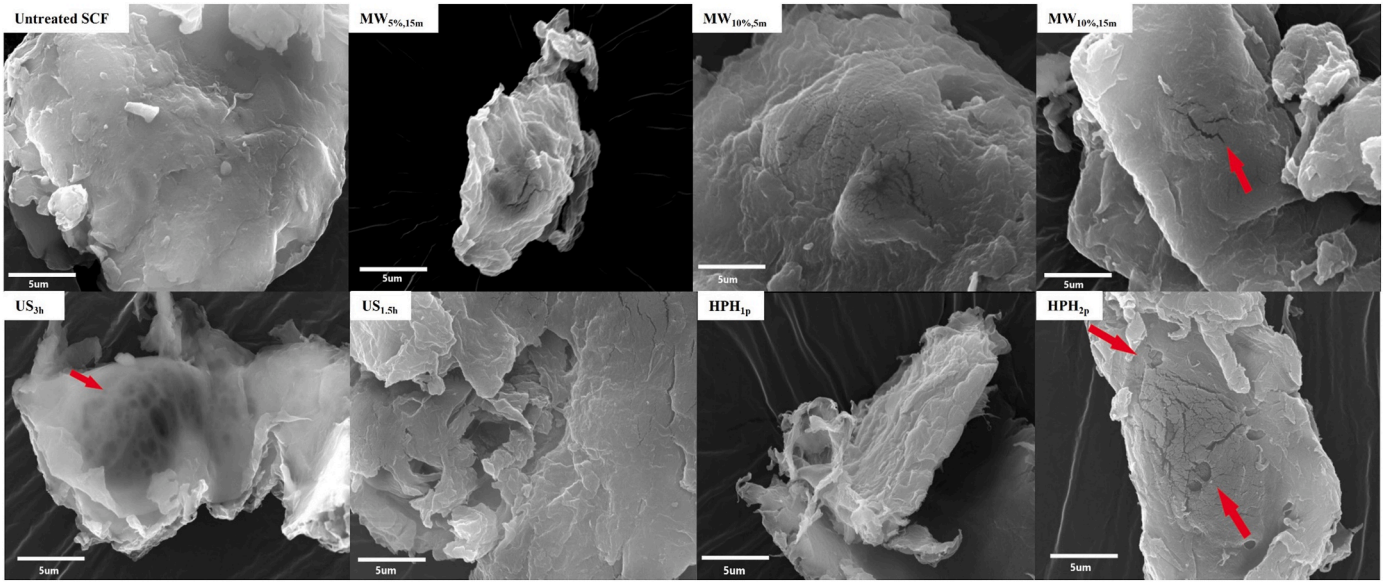

Fig. 2. SEM images of untreated and treated SCF samples. The red arrows highlight the cracks and/or holes observed on the surface of the treated SCF samples. (For interpretation of the references to color in this figure legend, the reader is referred to the Web version of this article.)

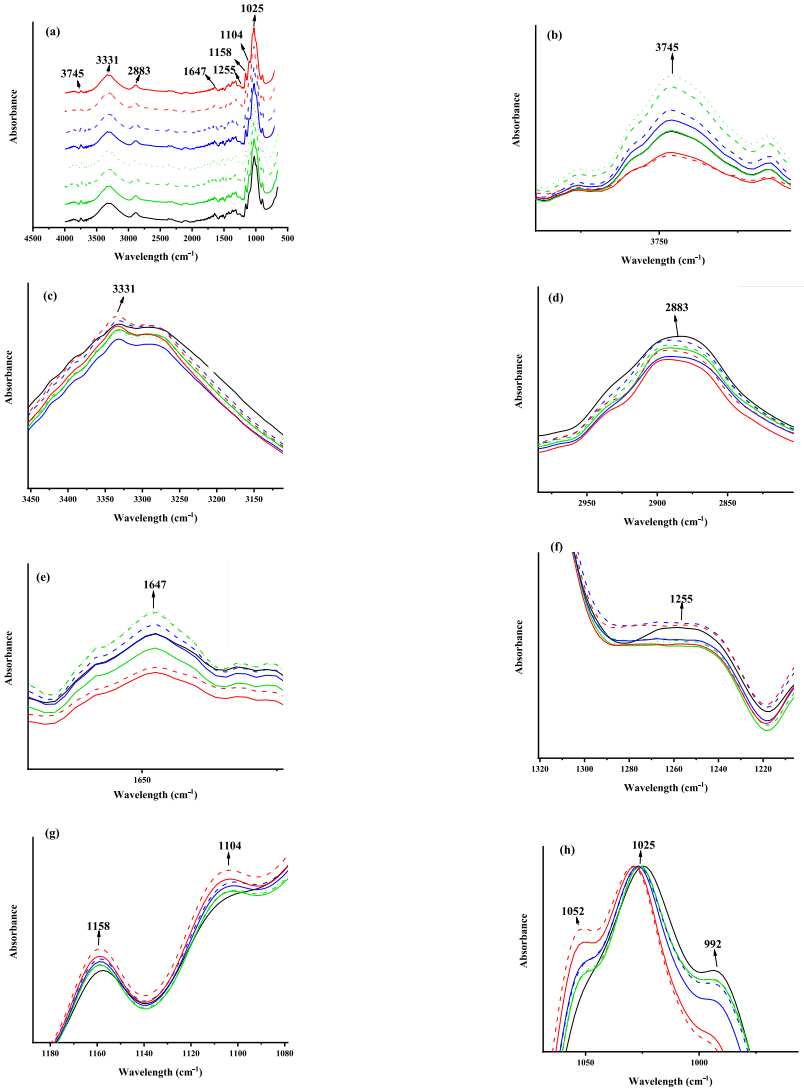

Fig. 3. a) Stacked plot FTIR spectra (500-4000 cm^{-1},) of SCFs before and after physical treatments (The curves were shifted vertically with respect to each other for a clearer presentation), b & c) OH stretching vibration area related to hydrogen bond formation at 3200-3800 cm^{-1}, c) The –CH stretching vibrations of cellulose at 2883 cm^{-1}, e) vibration of bound water molecules in hemicellulose at wavelength 1647 cm^{-1}, f) C═O stretching region at 1255 cm^{-1}, g) cellulose characteristic peaks at 1158 & 1104 cm^{-1} and g) fingerprint of hemicellulose corresponding to the skeletal vibration of C–O–C pyranose ring at 1052 & 1025 cm^{-1} and glycosidic C–H deformation of cellulose at 992 cm^{-1}.

degree of damage to the sample matrix can be milder, compared to high pressure homogenization, followed by microwave irradiation, which appeared as the mildest.

3.1.3. Surface morphology detected by SEM

Fig. 2 depicts the SEM images, a comparison between the untreated fibre to the treated fibres. SEM showed that the untreated fibre sample had a smooth and undamaged surface on most occasions, unlike the treated samples which showed variable degrees of disruption on the surface. When the fibre was pre-treated with microwave irradiation ($MW_{10\%,15m}$), slight cracks were observed on the surface, unlike the holes which formed on the surface when the fibre was ultrasonicated (US_{3h}). On the other hand, cracks and holes formed on the surface when the fibre underwent two passes with high pressure homogenization (HPH_{2p}). Similar observations were noted in the literature Wang et al. (2012), whereby porous surfaces were captured on peach and oat insoluble fibres that had undergone high pressure homogenization. Thus, it is possible that high pressure homogenization resulted in a greater damage to the sample structure, whereas less damage was caused by ultrasonication and, lastly, microwave irradiation being the mildest pretreatment out of the three methods. This can further support earlier results on WHC and OHC, whereby significant increases were reportedly noted with more extensive damage/disruption to the sample matrix. This enabled more entrapment, with pore formation by high pressure homogenization, as well as a greater exposure of functional groups.

3.1.4. FTIR

Fig. 3 depicts the FTIR spectra of untreated and physically treated SCFs. Typical absorption peaks include hydroxyl moieties (stretching vibrations of OH) at 3200–3800 cm^{-1}, C–H stretching vibration at 2883 cm^{-1}, O–H vibration of bound water at 1647 cm^{-1}, C–O stretching vibration at 1158 cm^{-1}, –COO at 1200–900 cm^{-1}, C–O–C vibration at 1024 cm^{-1}, and C–O–C stretching (β–(1, 4)–glycosidic linkage in cellulose) at 897 cm^{-1} (Cichosz & Masek, 2019; Ewulonu et al., 2019; Xie et al., 2016). The broadband in the 3000–3800 cm^{-1} region provided remarkable information to elaborate on the presence of hydrogen bonds. Variable degrees of hydrogen bonding and their interactions among hydroxyl groups occurred in the cellulose, hemicellulose and lignin, depicting wider characteristics in the OH stretching vibration area (3000-3800 cm^{-1}). In other words, the band position in hydrogen bond formation (3000-3800 cm^{-1}) was substantially related to the vibrational modes (free, inter- and intra-molecular hydroxyl groups), whereas the band intensity correlated with the population of hydrogen bonds (Schramm, 2020). When an OH group is free, the OH covalent bond is capable of absorption at high frequencies (3745 cm^{-1} for $MW_{10\%,5m}$ and

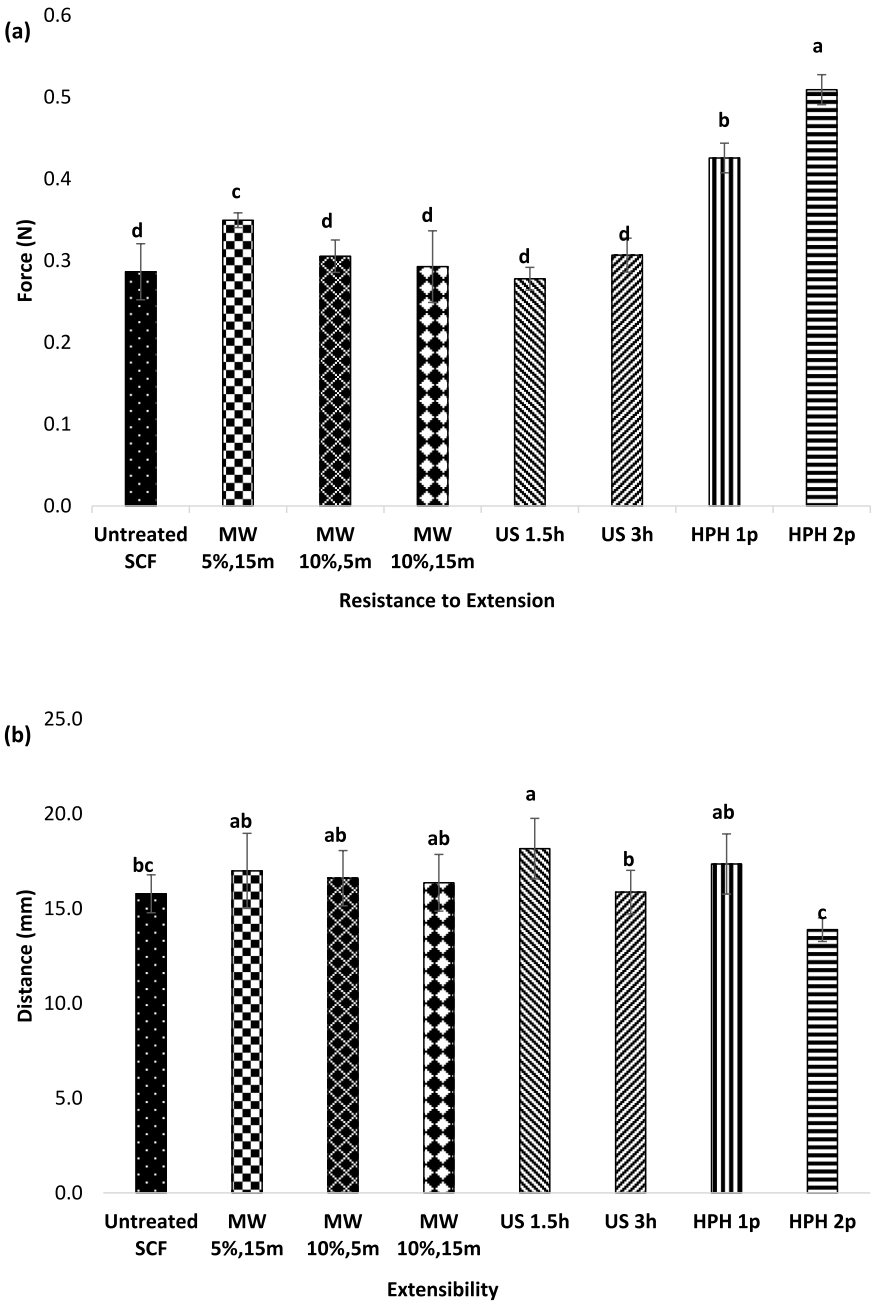

Fig. 4. a) Resistance to extension (N) (top) and b) Extensibility (mm) (bottom) of dough samples incorporated with 5% treated and untreated SCF, different letters represent a significant difference. refers to Untreated SCF sample, refers to $MW_{5\%,15m}$, refers to $MW_{10\%,5m}$, refers to $MW_{10\%,15m}$, refers to $US_{1.5h}$, refers to US_{3h}, refers to HPH_{1p}, and refers to HPH_{2p}.

$MW_{10\%,15m}$) as indicated in Fig. 3(b). The covalent bond is weakened and absorbs at lower frequencies when the same OH group participates in a hydrogen bond. The stronger the hydrogen bond, the weaker the covalent bond becomes. Based on the points above, physical treatments of SCFs ($MW_{10\%,5m}$, $MW_{10\%,15m}$, US_{3h} and $US_{1.5h}$) caused the band at 3745 cm^{-1} to shift to a higher intensity, which implies that the corresponding hydrogen bonds are weakened, whereas the free hydroxyl group is strengthened (Turki et al., 2018). However, Fig. 3(c) shows that HPH_{2p} and $US_{1.5h}$ increased the intensity of the peak at 3331 cm^{-1}, corresponding to hydrogen bonds, thereby indicating an increase in the relative amount of hydrogen bonding and a consequent enhancement in cellulosic crystallinity. A higher cellulose crystallinity is positively associated with higher hydrogen bond proportions (Zhao et al., 2009). Moving on, the absorption band at 2883 cm^{-1} was linked to C–H stretching vibrations from cellulose, which reportedly occurred in previous research as well, but shifting was not observed among treated SCFs (Fig. 3(d)). Notably, Fig. 3(e) indicates that the high-pressure homogenization treatment reduced the apparent peak intensity of 1647 cm^{-1}, representing the bending vibration of bound water molecules in hemicellulose. These findings suggest that the high-pressure homogenization treatment resulted in the loss of bound water molecules and caused a potential loss of hemicellulose. According to previous reports, the

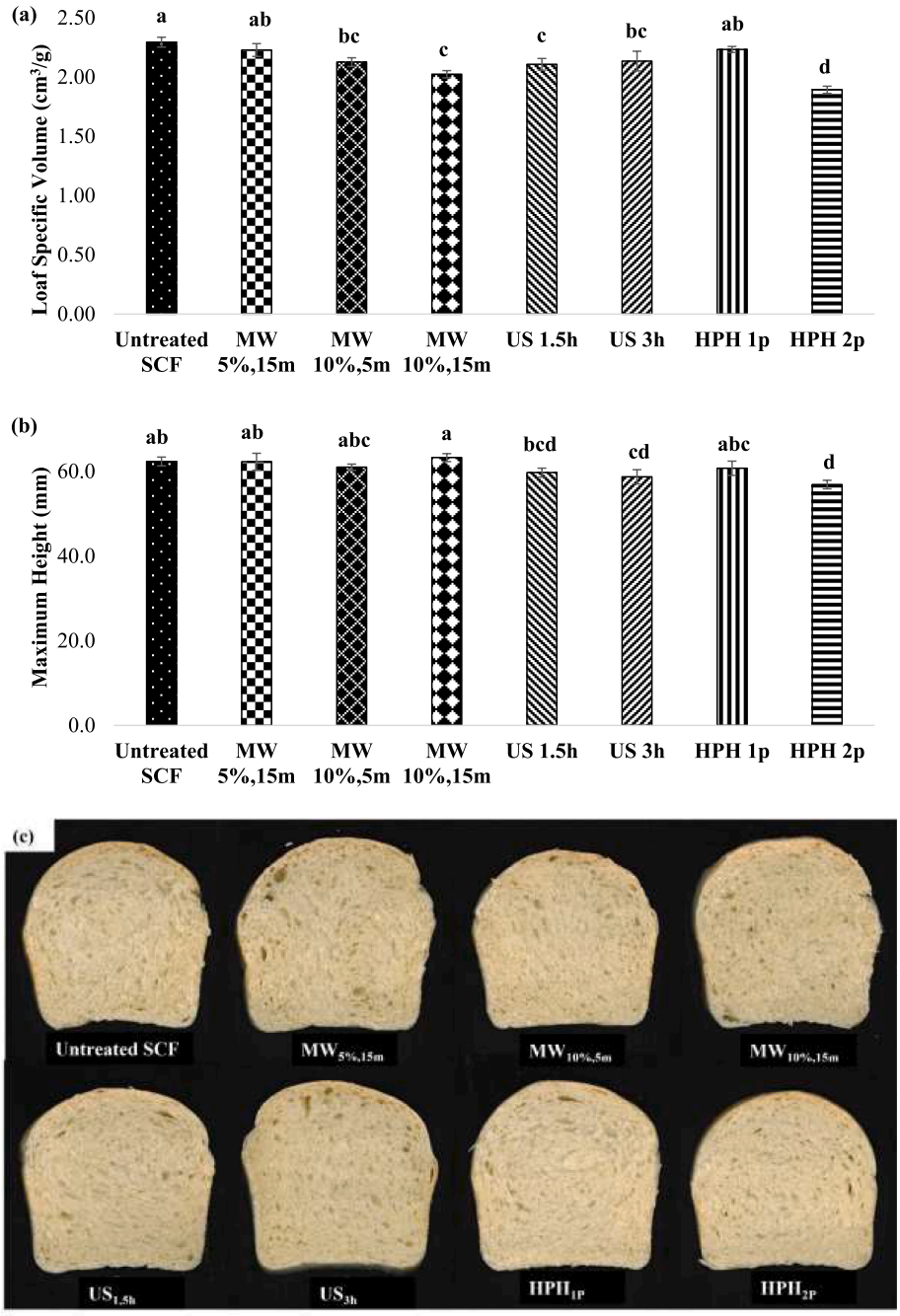

Fig. 5. (a) Specific loaf volume across bread formulations (top), where error bars represent mean ± SD (n = 4) and different letters indicate a significant difference ($p < 0.05$). (b) Maximum loaf height across bread formulations (middle), where error bars represent mean ± SD (n = 4) and different letters indicate a significant difference ($p < 0.05$). (c) Cross-sectional photographs illustrating the crumb appearance of bread samples.

removal of bound water can cause cellulosic hornification, resulting in lower reactivity and wettability as well as the collapse of the pore system, thereby confirming the SEM results in Fig. 2 (Song et al., 2021). The peak at 1255 cm^{-1} resulted from the C═O stretching in condensed guaiacyl units of lignin. The band in Fig. 3(f) indicated a significant decrease of intensity for the treated SCF. This observation indicated that the treatments caused lignin to slightly degrade. The peaks at 1104 cm^{-1} and 1158 cm^{-1} were identified for cellulose (Fig. 3(g)) (Esteves Costa et al., 2016; Ewulonu et al., 2019). In the case of untreated SCF, the peak at 1104 cm^{-1} was not notable, but the peaks occurred in treated SCF. The peak of 1158 cm^{-1} showed the shifting to a higher wavelength after the treatment, which meant that the physical treatment enhanced the cellulose characteristics in SCFs. The absorption peaks at 1025–1052 cm^{-1} can be regarded as the chemical fingerprint of hemicellulose, corresponding to the skeletal vibration of C–O–C pyranose ring (Fig. 3 (h)) (Rana et al., 2010). In other words, the presence of xylane and hemicellulose glycosidic linkages had associations with 1024–1052 cm^{-1} that correlated with stretching in the hydrogen bonding system. This region was shifted to a higher wavelength for the treated fibres, indicating reduced hemicellulose after applying all treatments (Merkel et al., 2014). The decrease in the spectral absorbance at 992 cm^{-1} correlated with ring vibration, revealing contributions to glycosidic C–H deformation of cellulose, as observed in all samples and, most obviously, in HPH_{1p} (Fig. 3(h)).

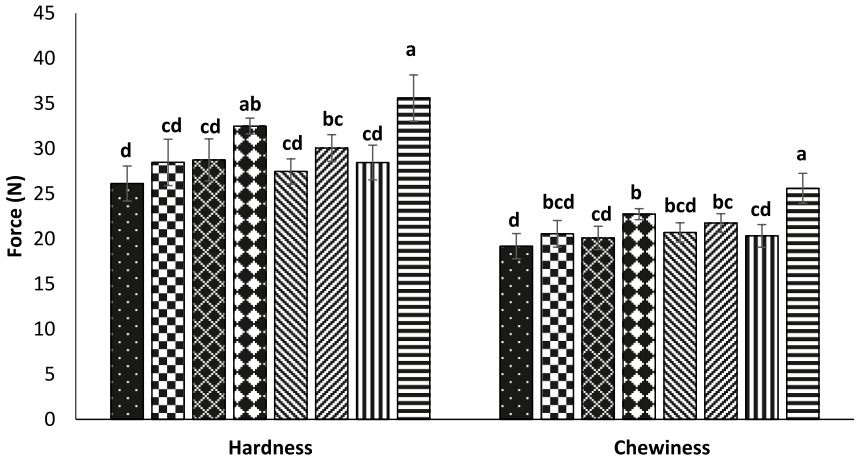

Fig. 6. Hardness and chewiness of bread at day 1 after baking and stored at room temperature. Error bars represent mean ± SD (n = 6), where different letters indicate a significant difference ($p < 0.05$) within the same texture attributes. refers to Untreated SCF sample, refers to $MW_{5\%,15m}$, refers to $MW_{10\%,5m}$, refers to $MW_{10\%,15m}$, refers to $US_{1.5h}$, refers to US_{3h}, refers to HPH_{1p}, and refers to HPH_{2p}.

3.2. Physical characterization of SCF-incorporated dough and bread

3.2.1. Effect of SCF incorporation on dough extensibility and bread texture

Fig. 4 shows the resistance to extension and extensibility of the dough samples collected after mixing. The untreated sample refers to the bread formulation with untreated SCF. According to the results, a significant increase was generally observed in the resistance to extension with the addition of treated SCF. The most significant increase in resistance to extension was observed when incorporating HPH_{2p}, followed by HPH_{1p}. The increase in dough stiffness was also reported in the literature (Ahmed et al., 2013) when wheat flour was substituted with insoluble date fibre. Generally, with the increase in resistance to extension, a decrease in dough extensibility was expected. This was the case with HPH_{2p}. However, with an enhanced resistance to extension and with reduced extensibility, the dough might not be fully able to entrap the gas that is produced during bread leavening and baking. In turn, this may affect the final loaf volume (Ma et al., 2021; Sangnark & Noomhorm, 2004). By adding fibre, the gas bubbles could collapse and coalesce, thereby reducing gas entrapment and causing a loss of loaf volume (Cavella et al., 2008).

3.2.2. Effect of SCF incorporation on maximum loaf height and specific loaf volume

The specific loaf volume, maximum loaf height and crumb appearance of the bread samples are depicted in Fig. 5. The lowest loaf specific volume and maximum height were observed in bread samples with HPH_{2p}. Other bread samples with SCF did not have any significant differences compared to the reference, apart from the $MW_{10\%,15m}$ and US_{3h} which had the next lowest loaf specific volumes. This could be due to a decrease in extensibility of the dough, as well as the dilution of gluten by adding SCF (Han et al., 2018). With the incorporation of sugarcane bagasse (Sangnark & Noomhorm, 2004), a reduced loaf volume was reported, along with an increase in fibre replacement levels due to the weakened ability of the dough for the retention of ferment-made gas. In a relevant study (Mudgil et al., 2016), the decrease in loaf specific volume occurred by gluten dilution when partially hydrolyzed guar gum was used as a substitute. From Fig. 6, most bread samples did not differ in terms of firmness, compared to the control sample. The bread sample with HPH_{2p} was the firmest, followed by $MW_{10\%,15m}$. This possibly resulted from an increase in the compactness of the samples when associated with reduced loaf volume and height. With the addition of fibre, the bread samples were reportedly more compact, had a reduced loaf volume, and exhibited greater loaf firmness (Ma et al., 2021; Sangnark & Noomhorm, 2004).

3.3. Effect of SCF incorporation on in vitro glycemic response of white bread

Fig. 7 shows the respective glycemic glucose equivalent (GGE) disposal, GGE release, and net GGE curves of the bread samples. Table 2 lists estimated values of the glycemic index (GI), which were calculated based on the iAUC, RGP, and RDS values. GI values are categorized as low (≤55), medium (55<GI < 70), and high (≥70) (Zhu, 2019). In this study, the estimated GI of white bread was assumed as 100. Based on Table S2, the total iAUC values of SCF-incorporated breads were lower than that of the reference sample. A similar trend was also observed in the RGP and RDS values. Similarly, as shown in Table 2, the estimated GI of SCF-incorporated breads were lower than that of the reference sample, thereby falling under the "medium" GI category. However, in general, the total iAUC, RDS, and estimated GI values among the SCF-incorporated bread are indifferent. This trend matches a study previously conducted by Seki et al. (2005) which showed that insoluble dietary fibers lowered the post-prandial blood glucose concentration. A previous study conducted by Sciarini et al. (2017) showed that adding oat fiber resulted in a decrease in the estimated GI value, possibly because of disruptions in the structure between starch and gluten. Water content was 45.3% in SCF-added bread formation while 38.5% for reference bread, as determined by a prior farinograph analysis. The additional amount of water in the SCF bread formula might enhanced starch gelatinization, or the concentration of 5% of SCF incorporated into the bread is low that the difference in treated SCF in controlling starch gelatinization is shadowed and therefore no significant difference was observed in all SCF incorporated breads. As farinograph is a commonly used tool in bakery industry to assess water content in developing dough formulation, unfoturatnely the treated SCF samples were not sufficient to incorporate higher amount of SCF into the bread to explore the impacts of HPH_{2p} SCF in bread texture and starch digestion at higher concentrations above 5%. The research team has done some preliminary studies to incorporate 10% untreated SCF into the bread but the textural and sensorial properties are not acceptable to local consumer and therefore higher concentrations of SCF was not conducted in this study, which is an area to explore for future studies if the SCF

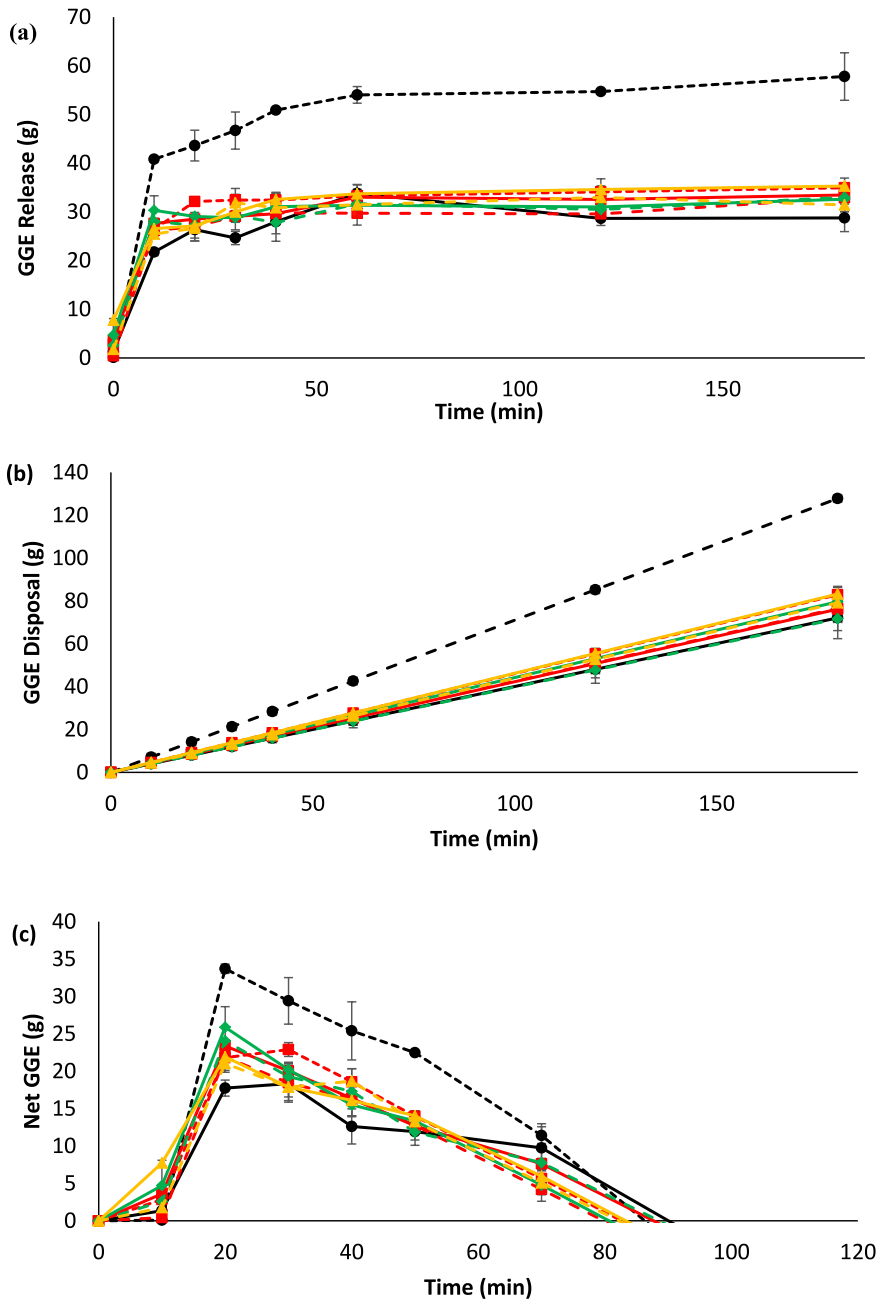

Fig. 7. (a) GGE release curves illustrating overall glucose release. (b) GGE disposal curves. (c) Net GGE curves. Error bars represent mean ± standard deviation (n = 2). All data were calculated based on the fresh weight of the bread samples without SCF incorporated (reference), incorporated with 5% untreated SCF, and modified SCF. refers to Reference, refers to Untreated SCF sample, refers to $MW_{5\%,15m}$, refers to $MW_{10\%,5m}$, refers to $MW_{10\%,15m}$, refers to $US_{1.5h}$, refers to US_{3h}, refers to HPH_{1p}, and refers to HPH_{2p}.

amount is not a limitation. Considering the experimental design used in this study has covered the commercialization aspects and therefore the results are relevant to the real-life application of SCF in white bread.

4. Conclusion

In this study, microwave, ultrasound, and high-pressure homogenization were used to modify SCF. In descriptive terms, SEM, FTIR, and light scattering particle analyzer techniques were applied to several aspects of analyses such as particle size, structure, functional groups, WHC, and OHC. The results revealed that after HPH_{2p} modification, it demonstrated the highest WHC and OHC. High OHC values were attributed to the presence of cracks and holes in the structure, as confirmed by SEM. Also, FTIR findings suggested that the physical treatments of SCFs enhanced the cellulosic part of fibres. Furthermore, HPH treatments caused the loss of bound water molecules and a potential loss of hemicellulose. Although the physical treatment positively affected the physicochemical properties, applying it to wheat flour-based dough might have a negative effect on textural properties. Dough and bread samples with HPH_{2p} exhibited lower values of dough extensibility, specific loaf volume, and height, which was associated with an increase in the hardness and chewiness of the bread. This resulted from the competition between SCF and gluten for the absorption of water, as HPH_{2p} had the highest WHC. Despite its impact on textural properties, adding the SCF to bread samples successfully lowered the estimated GI values of bread. Since the physical treatments had roles in improving the physicochemical properties of the SCF, and while considering their applicability in commercialization initiatives, future research can examine the other bakery products in this regard, with the potential application to manage blood sugar-related diseases.

Table 2
Estimated glycemic index (GI) values of bread samples with no incorporated SCF (reference), incorporated with 5% untreated SCF, and modified SCF, on a fresh weight basis.

Sample	Estimated GI		
	iAUC	RGP	RDS
Reference	100	100	100
Untreated	61	52	60
$MW_{5\%,15M}$	68	60	65
$MW_{10\%,5M}$	67	62	74
$MW_{10\%,15M}$	58	54	62
$US_{1.5H}$	66	57	67
US_{3H}	68	56	62
HPH_{1P}	66	63	62
HPH_{2P}	61	60	61

CRediT authorship contribution statement

Zawanah Abdol Rahim Yassin: Conceptualization, Methodology, Investigation, Visualization, Software, Writing – original draft. **Fatin Natasha Binte Abdul Halim:** Methodology, Investigation, Software, Visualization, Writing – original draft, Writing – review & editing. **Afsaneh Taheri:** Methodology, Investigation, Software, Visualization, Writing – review & editing. **Kelvin Kim Tha Goh:** Funding acquisition, Conceptualization, Methodology. **Juan Du:** Funding acquisition, Conceptualization, Methodology, Project administration, Supervision, Writing – review & editing.

Declaration of competing interest

The authors declare that they have no known competing financial interests or personal relationships that could have appeared to influence the work reported in this paper.

Data availability

Data will be made available on request.

Acknowledgments

This study was funded by Singapore Institute of Technology Ignition Grant (R-MOE-E103-F019), and Singapore Food Story R&D Programme Industry Alignment Fund Pre-positioning (IAF-PP) Theme 2—Advanced Biotech-based Protein Production Grant (A21H7a0131 and H21H8a0005), administered by A*STAR. We acknowledge the support by Tamu Group Pte Ltd, and would like to thank Dr. Enyi Ye and Ms. Casandra Chai from Institute of Materials Research and Engineering (IMRE), Agency for Science, Technology and Research, Singapore; the previous and present lab mates from Singapore Institute of Technology, Ms. Shanice Lim, Mr. Cedric Sow Wee Jian, Ms. Cheryl Ng Kwoek Zhen, Mr. Jeremy Chin Tak Gun, Dr. Zhao Lin and Mr. Lim Churn Hian for their kindness and assistance.

Appendix A. Supplementary data

Supplementary data to this article can be found online at https://doi.org/10.1016/j.lwt.2023.115008.

References

AACC International Approved Methods 54-21.02. (2011). Rheological behavior of flour by farinograph: Constant flour weight procedure. *AACC International Approved Methods, 54*, 1–8. https://doi.org/10.1094/AACCIntMethod-54-21.02, 21.02.

AACC International Method 10-05.01. (2001). Guidelines for measurement of volume by rapeseed displacement. In *AACC international method 10-05.01* (pp. 3–6). AACC International. https://doi.org/10.1094/aaccintmethod-10-05.01.

AACC International Method 10-09.01. (2009). Basic straight-dough bread-baking method–long fermentation. In *AACC international method 10-09.01* (pp. 1–6). AACC International. https://doi.org/10.1094/aaccintmethod-10-09.01.

Abdullah, M. M., Aldughpassi, A. D., Sidhu, J. S., Al-Foudari, M. Y., & Al-Othman, A. R. (2021). Effect of psyllium husk addition on the instrumental texture and consumer acceptability of high-fiber wheat pan bread and buns. *Annals of Agricultural Science, 66*(1), 75–80. https://doi.org/10.1016/j.aoas.2021.05.002

Agu, O., Tabil, L., & Dumonceaux, T. (2017). Microwave-Assisted alkali pre-treatment, densification and enzymatic saccharification of canola straw and oat hull. *Bioengineering, 4*(4), 25. https://doi.org/10.3390/bioengineering4020025

Ahmadi, S., Sheikh-Zeinoddin, M., Soleimanian-Zad, S., Alihosseini, F., & Yadav, H. (2019). Effects of different drying methods on the physicochemical properties and antioxidant activities of isolated acorn polysaccharides. *Lwt, 100*, 1–9. https://doi.org/10.1016/J.LWT.2018.10.027

Ahmed, J., Almusallam, A. S., Al-Salman, F., AbdulRahman, M. H., & Al-Salem, E. (2013). Rheological properties of water insoluble date fiber incorporated wheat flour dough. *LWT - Food Science and Technology, 51*(2), 409–416. https://doi.org/10.1016/J.LWT.2012.11.018

Alba, K., Rizou, T., Paraskevopoulou, A., Campbell, G. M., & Kontogiorgos, V. (2020). Effects of blackcurrant fibre on dough physical properties and bread quality characteristics. *Food Biophysics, 15*(3), 313–322. https://doi.org/10.1007/S11483-020-09627-X

Ameram, N., Muhammad, S., Nik Yusof, N. A. A., Ishak, S., Ali, A., Shoparwe, N. F., & Ter, T. P. (2019). Chemical composition in sugarcane bagasse: Delignification with sodium hydroxide. *Malaysian Journal of Fundamental and Applied Sciences, 15*(2), 232–236. https://doi.org/10.11113/MJFAS.V15N2.1118

Atkinson, F. S., Foster-Powell, K., & Brand-Miller, J. C. (2008). International tables of glycemic index and glycemic load values: 2008. *Diabetes Care, 31*(12), 2281–2283. https://doi.org/10.2337/dc08-1239

Baena-Díez, J. M., Peñafiel, J., Subirana, I., Ramos, R., Elosua, R., Marín-Ibañez, A., Guembe, M. J., Rigo, F., Tormo-Díaz, M. J., Moreno-Iribas, C., Cabré, J. J., Segura, A., García-Lareo, M., Cámara, A. G. de la, Lapetra, J., Quesada, M., Marrugat, J., Medrano, M. J., Berjón, J., … Grau, M. (2016). Risk of cause-specific death in individuals with diabetes: A competing risks analysis. *Diabetes Care, 39*(11), 1987–1995. https://doi.org/10.2337/DC16-0614

Binte Abdul Halim, F. N., Taheri, A., Abdol Rahim Yassin, Z., Chia, K. F., Goh, K. K. T., Goh, S. M., & Du, J. (2023). Effects of incorporating alkaline hydrogen peroxide treated sugarcane fibre on the physical properties and glycemic potency of white bread. *Foods, 12*(7), 1460. https://doi.org/10.3390/foods12071460

Borczak, B., Sikora, M., Sikora, E., Dobosz, A., & Kapusta-Duch, J. (2018). Glycaemic index of wheat bread. *Starch/Staerke, 70*(1–2), Article 1700022. https://doi.org/10.1002/star.201700022

Brahim, M., El Kantar, S., Boussetta, N., Grimi, N., Brosse, N., & Vorobiev, E. (2016). Delignification of rapeseed straw using innovative chemo-physical pretreatments. *Biomass and Bioenergy, 95*, 92–98. https://doi.org/10.1016/J.BIOMBIOE.2016.09.019

Burton, P., Monro, J. A., Alvarez, L., & Gallagher, E. (2011). Glycemic impact and health: New horizons in white bread formulations. *Critical Reviews in Food Science and Nutrition, 51*(10), 965–982. https://doi.org/10.1080/10408398.2010.491584

Cavella, S., Romano, A., Giancone, T., & Masi, P. (2008). The influence of dietary fibres on bubble development during bread making. In *Bubbles in food 2: Novelty, Health and luxury* (Vols. 311–321). https://doi.org/10.1016/B978-1-891127-59-5.50035-3

Chen, J., Gao, D., Yang, L., & Gao, Y. (2013). Effect of microfluidization process on the functional properties of insoluble dietary fiber. *Food Research International, 54*(2), 1821–1827. https://doi.org/10.1016/J.FOODRES.2013.09.025

Cichosz, S., & Masek, A. (2019). Cellulose fibers hydrophobization via a hybrid chemical modification. *Polymers, 11*(7), 1174. https://doi.org/10.3390/POLYM11071174

Dickinson, E. (2018). Hydrocolloids acting as emulsifying agents – how do they do it? *Food Hydrocolloids, 78*, 2–14. https://doi.org/10.1016/J.FOODHYD.2017.01.025

Ellis, P. R., Roberts, F. G., Low, A. G., & Morgan, L. M. (1995). The effect of high-molecular-weight guar gum on net apparent glucose absorption and net apparent insulin and gastric inhibitory polypeptide production in the growing pig: Relationship to rheological changes in jejunal digesta. *British Journal of Nutrition, 74*(4), 539–556. https://doi.org/10.1079/bjn19950157

Esteves Costa, C. A., Coleman, W., Dube, M., Rodrigues, A. E., & Rodrigues Pinto, P. C. (2016). Assessment of key features of lignin from lignocellulosic crops: Stalks and roots of corn, cotton, sugarcane, and tobacco. *Industrial Crops and Products, 92*, 136–148. https://doi.org/10.1016/J.INDCROP.2016.07.032

Ewulonu, C. M., Liu, X., Wu, M., & Huang, Y. (2019). Ultrasound-assisted mild sulphuric acid ball milling preparation of lignocellulose nanofibers (LCNFs) from sunflower stalks (SFS). *Cellulose, 26*(7), 4371–4389. https://doi.org/10.1007/S10570-019-02382-4

Gould, J. M., Jasberg, B. K., Dexter, L. B., Hsu, J. T., Lewis, S. M., & Fahey, G. C. (1989). High-fiber, noncaloric flour substitute for baked foods. Properties ofalkaline peroxide-treated lignocellulose. *Cereal Chemistry, 66*(3), 201–205.

Han, W., Ma, S., Li, L., Zheng, X., & Wang, X. (2018). Rheological properties of gluten and gluten-starch model doughs containing wheat bran dietary fibre. *International Journal of Food Science and Technology, 53*(12), 2650–2656. https://doi.org/10.1111/ijfs.13861

Hua, X., Xu, S., Wang, M., Chen, Y., Yang, H., & Yang, R. (2017). Effects of high-speed homogenization and high-pressure homogenization on structure of tomato residue fibers. *Food Chemistry, 232*, 443–449. https://doi.org/10.1016/J.FOODCHEM.2017.04.003

Kaack, K., Pedersen, L., Laerke, H. N., & Meyer, A. (2006). New potato fibre for improvement of texture and colour of wheat bread. *European Food Research and Technology, 224*, 199–207. https://doi.org/10.1007/s00217-006-0301-5

Kim, Y. A., Keogh, J. B., & Clifton, P. M. (2016). Polyphenols and glycémie control. *Nutrients, 8*(1). https://doi.org/10.3390/nu8010017. MDPI AG.

Lin, D., Xiao, M., Zhao, J., Li, Z., Xing, B., Li, X., Kong, M., Li, L., Zhang, Q., Liu, Y., Chen, H., Qin, W., Wu, H., & Chen, S. (2016). An overview of plant phenolic compounds and their importance in human nutrition and management of type 2 diabetes. *Molecules, 21*(10). https://doi.org/10.3390/molecules21101374. MDPI AG.

Liu, W., Brennan, M., Serventi, L., & Brennan, C. (2017). Buckwheat flour inclusion in Chinese steamed bread: Potential reduction in glycemic response and effects on dough quality. *European Food Research and Technology, 243*, 727–734. https://doi.org/10.1007/s00217-016-2786-x

Livesey, G., Taylor, R., Hulshof, T., & Howlett, J. (2008). Glycemic response and health - a systematic review and meta-analysis: Relations between dietary glycemic properties and health outcomes. *American Journal of Clinical Nutrition, 87*(suppl), 258S–268S. https://doi.org/10.1093/ajcn/87.1.258s

Lu, Z. H., Donner, E., & Liu, Q. (2021). Development and characterisation of gluten-free potato bread. *International Journal of Food Science and Technology, 56*(6), 3085–3098. https://doi.org/10.1111/ijfs.14952

Ma, S., Wang, Z., Liu, N., Zhou, P., Bao, Q., & Wang, X. (2021). Effect of wheat bran dietary fibre on the rheological properties of dough during fermentation and Chinese steamed bread quality. *International Journal of Food Science and Technology, 56*(4), 1623–1630. https://doi.org/10.1111/ijfs.14781

Merkel, K., Rydarowski, H., Kazimierczak, J., & Bloda, A. (2014). Processing and characterization of reinforced polyethylene composites made with lignocellulosic fibres isolated from waste plant biomass such as hemp. *Composites Part B: Engineering, 67*, 138–144. https://doi.org/10.1016/J.COMPOSITESB.2014.06.007

Mishra, S., Hardacre, A., & Monro, J. (2012). Food structure and carbohydrate digestibility. *Carbohydrates - Comprehensive Studies on Glycobiology and Glycotechnology*, 289–316. https://doi.org/10.5772/51969

Monro, J. A., Mishra, S. S., & Hardacre, A. (2011). Glycaemic impact regulation based on progressive geometric changes in solid starch-based food particles during digestion. *Food Digestion, 2*, 1–12. https://doi.org/10.1007/s13228-011-0009-2

Monro, J. A., Mishra, S., & Venn, B. (2010). Baselines representing blood glucose clearance improve in vitro prediction of the glycaemic impact of customarily consumed food quantities. *British Journal of Nutrition, 103*(2), 295–305. https://doi.org/10.1017/S0007114509991632

Mood, S. H., Golfeshan, A. H., Tabatabaei, M., Jouzani, G. S., Najafi, G. H., Gholami, M., & Ardjmand, M. (2013). Lignocellulosic biomass to bioethanol, a comprehensive review with a focus on pretreatment. *Renewable and Sustainable Energy Reviews, 27*, 77–93. https://doi.org/10.1016/J.RSER.2013.06.033

Mudgil, D., Barak, S., & Khatkar, B. S. (2016). Optimization of bread firmness, specific loaf volume and sensory acceptability of bread with soluble fiber and different water levels. *Journal of Cereal Science, 70*, 186–191. https://doi.org/10.1016/J.JCS.2016.06.009

Ognean, C. (2015). Technological and sensorial effects of sorghum addition at wheat bread. *Agriculture and Food, 3*, 209–217, 10.3/JQUERY-UI.JS.

Rabemanolontsoa, H., & Saka, S. (2016). Various pretreatments of lignocellulosics. *Bioresource Technology, 199*, 83–91. https://doi.org/10.1016/J.BIORTECH.2015.08.029

Rana, R., Langenfeld-Heyser, R., Finkeldey, R., & Polle, A. (2010). FTIR spectroscopy, chemical and histochemical characterisation of wood and lignin of five tropical timber wood species of the family of Dipterocarpaceae. *Wood Science and Technology, 44*(2), 225–242. https://doi.org/10.1007/S00226-009-0281-2/

Rosa-Sibakov, N., Sibakov, J., Lahtinen, P., & Poutanen, K. (2015). Wet grinding and microfluidization of wheat bran preparations: Improvement of dispersion stability by structural disintegration. *Journal of Cereal Science, 64*, 1–10. https://doi.org/10.1016/J.JCS.2015.04.002

Sangnark, A., & Noomhorm, A. (2004). Effect of dietary fiber from sugarcane bagasse and sucrose ester on dough and bread properties. *LWT - Food Science and Technology, 37*(7), 697–704. https://doi.org/10.1016/J.LWT.2004.02.015

Scazzina, F., Siebenhandl-Ehn, S., & Pellegrini, N. (2013). The effect of dietary fibre on reducing the glycaemic index of bread. *British Journal of Nutrition, 109*(7), 1163–1174. https://doi.org/10.1017/S0007114513000032

Schramm, C. (2020). High temperature ATR-FTIR characterization of the interaction of polycarboxylic acids and organotrialkoxysilanes with cellulosic material. *Spectrochimica Acta Part A: Molecular and Biomolecular Spectroscopy, 243*, Article 118815. https://doi.org/10.1016/J.SAA.2020.118815

Sciarini, L. S., Bustos, M. C., Vignola, M. B., Paesani, C., Salinas, C. N., & Pérez, G. T. (2017). A study on fibre addition to gluten free bread: Its effects on bread quality and in vitro digestibility. *Journal of Food Science and Technology, 54*(1), 244–252. https://doi.org/10.1007/s13197-016-2456-9

Seki, T., Nagase, R., Torimitsu, M., Yanagi, M., Ito, Y., Kise, M., Mizukuchi, A., Fujimura, N., Hayamizu, K., & Ariga, T. (2005). Insoluble fiber is a major constituent responsible for lowering the post-prandial blood glucose concentration in the pre-germinated brown rice. *Biological and Pharmaceutical Bulletin, 28*(8), 1539–1541. https://doi.org/10.1248/bpb.28.1539

Serra, M., Trujillo, A. J., Jaramillo, P. D., Guamis, B., & Ferragut, V. (2008). Ultra-high pressure homogenization-induced changes in skim milk: Impact on acid coagulation properties. *Journal of Dairy Research, 75*(1), 69–75. https://doi.org/10.1017/S0022029907003032

Shahi, N., Min, B., Sapkota, B., & Rangari, V. K. (2020). Eco-friendly cellulose nanofiber extraction from sugarcane bagasse and film fabrication. *Sustainability, 12*, 1–15. https://doi.org/10.3390/su12156015

Song, P., Zhou, F., Li, F., Han, Z., Wang, L., Xu, J., Zhang, B., Wang, M., Fan, J., & Zhang, B. (2021). Superfine pulverisation pretreatment to enhance crystallinity of cellulose from Lycium barbarum L. leaves. *Carbohydrate Polymers, 253*, Article 117207. https://doi.org/10.1016/J.CARBPOL.2020.117207

SRV, A., Mishra, S., Hardacre, A., Matia-Merino, L., Goh, K., Warren, F., & Monro, J. (2019). Kernel structure in breads reduces in vitro starch digestion rate and estimated glycaemic potency only at high grain inclusion rates. *Food Structure, 21*, Article 100109. https://doi.org/10.1016/j.foostr.2019.100109

Sultanova, N., Kasarova, S., & Nikolov, I. (2009). Dispersion properties of optical polymers. *Acta Physica Polonica A, 116*(4), 585–587. https://doi.org/10.12693/APhysPolA.116.585

Taheri, A., Kashaninejad, M., Tamaddon, A. M., Du, J., & Jafari, S. M. (2023). Rheological characteristics of soluble cress seed mucilage and β-lactoglobulin complexes with salts addition: rheological evidence of structural rearrangement. *Gels, 9*(6), 485. https://doi.org/10.3390/gels9060485

Tseng, C.-H. (2004). Mortality and causes of death in a national sample of diabetic patients in taiwan. *Diabetes Care, 27*(7), 1605–1609. https://doi.org/10.2337/DIACARE.27.7.1605

Turki, A., El Oudiani, A., Msahli, S., & Sakli, F. (2018). Investigation of OH bond energy for chemically treated alfa fibers. *Carbohydrate Polymers, 186*, 226–235. https://doi.org/10.1016/J.CARBPOL.2018.01.030

Vlachos, D., Malisova, S., Lindberg, F. A., & Karaniki, G. (2020). Glycemic index (GI) or glycemic load (GL) and dietary interventions for optimizing postprandial hyperglycemia in patients with T2 diabetes: A review. *Nutrients, 12*(6), 1561. https://doi.org/10.3390/nu12061561

Wang, J., Rosell, C. M., & Benedito de Barber, C. (2002). Effect of the addition of different fibres on wheat dough performance and bread quality. *Food Chemistry, 79*(2), 221–226. https://doi.org/10.1016/S0308-8146(02)00135-8

Wang, T., Sun, X., Zhou, Z., & Chen, G. (2012). Effects of microfluidization process on physicochemical properties of wheat bran. *Food Research International, 48*(2), 742–747. https://doi.org/10.1016/J.FOODRES.2012.06.015

Wang, F., Zeng, J., Gao, H., & Sukmanov, V. (2021). Effects of different physical technology on compositions and characteristics of bean dregs. *Innovative Food Science & Emerging Technologies, 73*, Article 102789. https://doi.org/10.1016/J.IFSET.2021.102789

Xie, J., Hse, C. Y., De Hoop, C. F., Hu, T., Qi, J., & Shupe, T. F. (2016). Isolation and characterization of cellulose nanofibers from bamboo using microwave liquefaction combined with chemical treatment and ultrasonication. *Carbohydrate Polymers, 151*, 725–734. https://doi.org/10.1016/J.CARBPOL.2016.06.011

Zhao, L., Chen, M., Bi, X., & Du, J. (2023). *Physicochemical properties, structural characteristics and in vitro digestion of brown rice–pea protein isolate blend treated by microbial transglutaminase*. Food Hydrocolloids. https://doi.org/10.1016/j.foodhyd.2023.108673, 108673, ISSN 0268-005X.

Zhao, H., Jones, C. L., Baker, G. A., Xia, S., Olubajo, O., & Person, V. N. (2009). Regenerating cellulose from ionic liquids for an accelerated enzymatic hydrolysis. *Journal of Biotechnology, 139*(1), 47–54. https://doi.org/10.1016/J.JBIOTEC.2008.08.009

Zhu, F. (2019). Glycemic control in Chinese steamed bread: Strategies and opportunities. *Trends in Food Science & Technology, 86*, 252–259. https://doi.org/10.1016/J.TIFS.2019.02.038

Zhu, X., Lundberg, B., Cheng, Y., Shan, L., Xing, J., Peng, P., Chen, P., Huang, X., Li, D., & Ruan, R. (2018). Effect of high-pressure homogenization on the flow properties of citrus peel fibers. *Journal of Food Process Engineering, 41*(3), Article e12659. https://doi.org/10.1111/JFPE.12659